



RESEARCH LETTER

10.1002/2014GL061934

Key Points:

- Hurricane eyewall can be studied from seismic amplitude versus distance plots
- Seismically derived surface pressure shows the location and strength of eyewall
- Time evolution of this decaying process can be tracked

Supporting Information:

- Readme
- Figure S1
- Figure S2

Correspondence to:

T. Tanimoto,
toshiro@geol.ucsb.edu

Citation:

Tanimoto, T., and A. Lamontagne (2014), Temporal and spatial evolution of an on-land hurricane observed by seismic data, *Geophys. Res. Lett.*, *41*, 7532–7538, doi:10.1002/2014GL061934.

Received 18 SEP 2014

Accepted 18 OCT 2014

Accepted article online 22 OCT 2014

Published online 12 NOV 2014

Temporal and spatial evolution of an on-land hurricane observed by seismic data

Toshiro Tanimoto¹ and Anne Lamontagne¹¹Department of Earth Science and Earth Research Institute, University of California, Santa Barbara, California, USA

Abstract A dense seismic array can provide new perspectives for a decaying hurricane after its landfall. The case of Hurricane Isaac in 2012 is presented using a seismic array from EarthScope (USArray). The amplitude-distance plots from the center of the hurricane showed a sharp peak at a distance of 75 km at the time of landfall. This peak decayed and moved outward from the center over the next 1.5 days. The sharp peak can be explained by strong surface pressure fluctuations under the eyewall in which a focused ascending flow is known to exist. We reconstructed the time evolution of surface pressure that explains seismic data. Pressure solutions indicate that the eyewall stayed at 75 km in the first 10 h after the landfall, while the ascending flow weakened significantly. In the following 24 h, the eyewall diffused and moved to distances about 200–300 km, suggesting its collapse during this period.

1. Introduction

After its landfall, a hurricane (tropical cyclone) quickly loses energy because there is no more influx of energy from the ocean. But how long and what level of strength it maintains after its landfall are important on the damage it inflicts upon the areas of the landfall and in the neighborhood of its path in the following 1–2 days. In this paper, we demonstrate that a dense seismological array can provide some insights into this decaying process of a hurricane.

Hurricane Isaac in 2012 was a tropical cyclone that was a tropical storm for most of its life [Berg, 2013]. It intensified to become a hurricane at about 12:00 UTC 28 August, 12 h before its first landfall at the mouth of the Mississippi River, and remained a hurricane until about 18:00 UTC 29 August (Figure 1). Its first landfall occurred at 00:00 UTC 29 August, but the eye went back to the nearby ocean. The second landfall occurred at 08:00 UTC 29 August, just west of Port Fourchon, Louisiana. After the second landfall, it moved northward in an area densely instrumented by seismographs by the EarthScope project (www.earthscope.org). EarthScope (USArray) was designed to study the interior of the Earth, but in this case, it happened to provide an excellent data set for studying this hurricane.

In this study, we only analyzed vertical component seismic data. All results and insights obtained are based on the analysis of vertical component seismograms. Also, hereafter, when we refer to the landfall, we refer to the second landfall at 08:00 UTC on 29 August.

2. Seismic Data Analysis: Frequency Band Selection

One of the difficulties in studying the strength of a hurricane by seismic waves is the fact that not all seismic waves come directly from the center of a hurricane. For some frequency bands, ocean waves, which are excited by strong winds by the same hurricane, become secondary sources of seismic wave excitation, and they may have stronger influences than the processes near the center of a hurricane. It is now well understood how ocean waves can generate seismic waves through its direct interaction with the solid Earth at sea bottom [Hasselmann, 1963] as well as their mutual collisions [Longuet-Higgins, 1950]. For a storm on the east coast of the United States, for example, Bromirski [2001] showed that seismic waves in the microseismic frequency bands (0.05–0.3 Hz) actually come from near-coastal oceans rather than directly from the center of a storm. In order to study the processes near the center of a hurricane, we should avoid using those seismic waves generated by ocean waves.

An answer to this problem turned out to be in the selection of frequency bands. By examining seismic wave amplitudes at various frequencies, we learned that processes near the hurricane eye are the dominant source of low-frequency seismic waves about 0.01–0.02 Hz, but ocean waves are far more important sources for

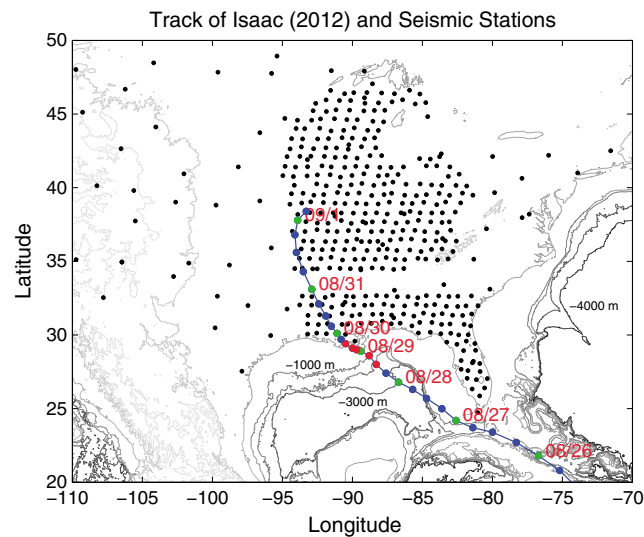


Figure 1. Track of Hurricane Isaac (August 2012) and seismic stations from EarthScope (solid circles). The blue circles indicate when Isaac was a tropical storm, the red circles indicate its hurricane stage, and the green circles are the day markers (00:00 UTC for each day).

hurricane. Clearly, these seismic waves in the frequency range of 0.24–0.25 Hz are excited in the ocean. In general, we found that waves at higher frequencies than 0.1 Hz are excited more efficiently in the ocean and do not generally come from the center of a hurricane. Therefore, in order to study the processes near the hurricane eye, we chose to focus on the frequency range of 0.01–0.02 Hz.

3. Amplitude-Distance Plot From Hurricane Center

In Figures 3b–3g, we show how the amplitudes for the frequency range of 0.01–0.02 Hz varied with distance from the center of the hurricane. These plots are the snapshots of the amplitude-distance plots at the 4th, 10th, 16th, 22nd, 28th, and 34th hour after the landfall. Spectral amplitudes were computed using the Hanning window and fast Fourier transform and the time series length of 1 h for each case. Then spectral amplitudes were averaged for the frequency range between 0.01 and 0.02 Hz.

Around the time of landfall (and until the 4th hour), the amplitude peak is sharp and is located at a distance (radius) about 75 km from the center (Figure 3b). A vertical short line is given at the top of each panel to indicate the distance of 75 km. At the 10th hour (Figure 3c), the peak value had decreased by a factor of 2, and the width of the peak became slightly broader, but the peak location stayed at about the same distance from the hurricane center. The peak for the 16th hour still stayed close (Figure 3d), but there is clear indication that the width of the peak had increased. At the 22nd hour (Figure 3e) and the 28th hour (Figure 3f), the widths of the peak became much wider with increased scatter in seismic amplitudes. The peak radius also increased clearly. At the 34th hour (Figure 3g), a broad peak at a distance of about 300 km can be recognized, but the scatter is large from the center to a distance of about 400 km.

These changes in seismic amplitudes must be related to the manner in which a hurricane lost its energy after the landfall. The vertical flow in the eyewall was confirmed before [e.g., Jorgensen, 1984; Jorgensen et al., 1985], but Emanuel [1986, 1991, 1997] pointed out that in a mature hurricane, there is a Carnot-cycle-like process as sketched in Figure 3a. Leg 1 in this panel shows an inflow of air that spirals into the center of the hurricane. Once the air reaches the point where the wind velocity reaches its maximum, the airflow turns upward along Leg 2. This is the ascending flow in the eyewall. At the top of the troposphere, the air flows outward from the center and then goes down along Leg 3 and Leg 4 back to the surface of the Earth. The ascending flow of air along Leg 2 can be quite intense when a hurricane is strong and probably cause large pressure changes on the surface of the Earth. It seems most natural to assume that the time evolution of amplitude-distance data in Figures 3b–3g is caused by surface pressure changes and is related to the decay of this hurricane.

higher-frequency waves above 0.1 Hz. Figure 2 shows two examples of seismic amplitudes at EarthScope stations; Figure 2a is an example for the low-frequency seismic waves (0.01–0.02 Hz); the location of the hurricane center is shown by the red triangle [Berg, 2013], and the concentric circles from the center are drawn at every 100 km. Amplitudes plotted against distance from the hurricane center are shown in the bottom. In Figure 2a, high-amplitude stations (red) tend to surround the center with similar distances to it. This is not the case for high-frequency waves in Figure 2b (0.24–0.25 Hz). In this case, stations with high amplitudes are found only on the southside of the center and are primarily located near the coast. In fact, as the arrow in the bottom of Figure 2b indicates, amplitudes decrease from the coast toward the center of the

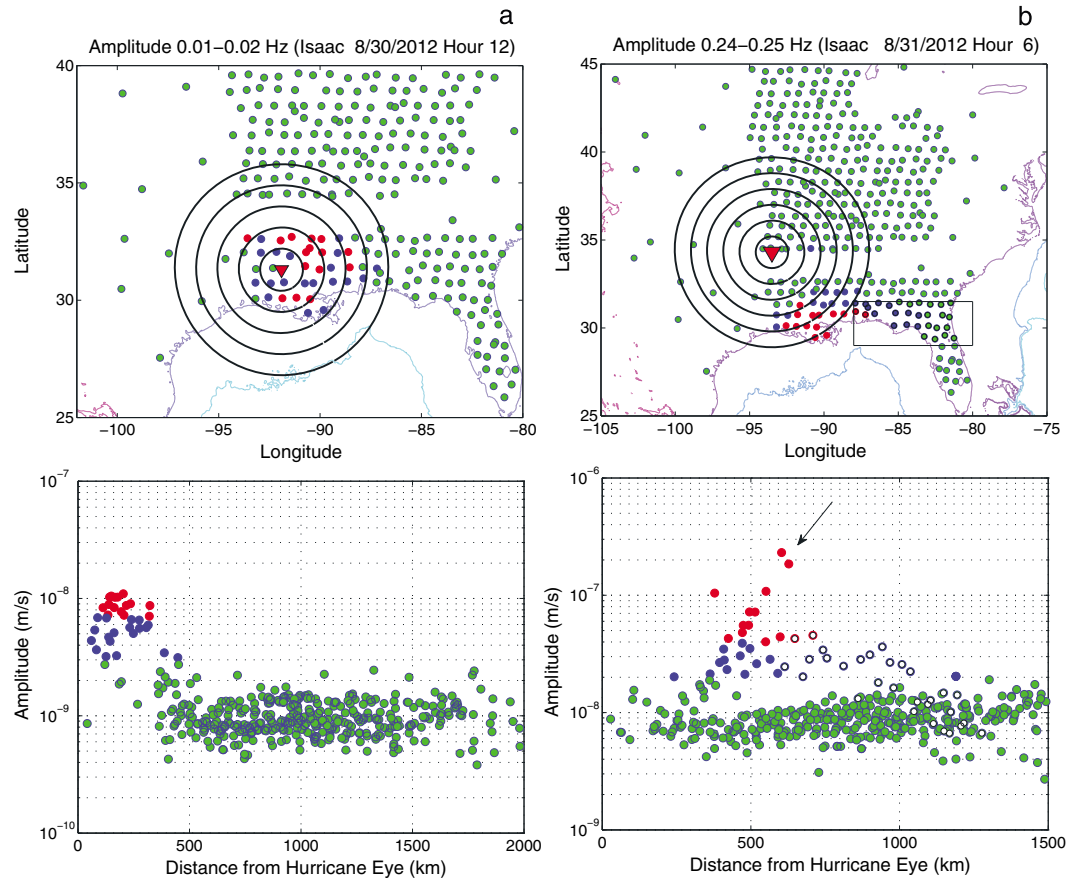


Figure 2. Seismic amplitudes and locations of Hurricane Isaac. Locations of the hurricane are indicated by the red triangles. The top row shows the seismic amplitudes on a map in three colors, and the bottom row shows the amplitude-distance plot from the center of the hurricane (red triangle). The concentric circles are given for every 100 km from the center. (a) Most of seismic waves between 0.01 and 0.02 Hz that emanate from the center of the hurricane as high-amplitude stations (red and blue) are found within the same concentric circles. The red circles indicate amplitudes higher than 7.0×10^{-9} (m/s), the blue circles are between 3.0×10^{-9} and 7.0×10^{-9} (m/s), and green circles are below 3.0×10^{-9} (m/s). (b) The seismic waves between 0.24 and 0.25 Hz. The highest amplitudes are found near the coast (red), and the arrow in the bottom indicates that the amplitudes decreased from the coast toward the center of the hurricane. Stations in northern Florida, within the rectangular box in the top, are shown by the white circles in the bottom and indicate that these near-coastal stations also have anomalously high amplitudes.

4. Random Surface Pressure Source and Modeling

The amplitude-distance data, as shown in Figures 3b–3g, are basically the raw seismic data, and the locations of the excitation sources must be obtained from them. We postulate that these seismic waves were generated by surface pressure fluctuations and solved for the time evolution of surface pressure that can explain the seismic data in Figures 3b–3g. We formulate this analysis as an inverse problem of seismic data for the surface pressure fluctuations and examine how the excitation sources changed over time after the landfall.

We assume random pressure sources that are distributed on the surface and are characterized by two parameters: its strength (pressure power spectral density or hereafter pressure PSD) and the correlation length. We also assume that the pressure PSD is axisymmetric as a hurricane may be regarded axisymmetric to first order.

The basic equation for this inverse problem can be derived in a similar manner to *Fukao et al.* [2002] and *Tanimoto* [2005], obtained for slightly different problems. It has the form

$$S_v(x, \omega) = \int K(x, x_s, \omega) S_p(x_s, \omega) dx_s \tag{1}$$

where $S_v(x, \omega)$ is the PSD of observed seismic ground velocity at distance x from the center of the hurricane (angular frequency ω), $S_p(x_s, \omega)$ is the surface pressure PSD that we solve for, and $K(x, x_s, \omega)$ is the inversion

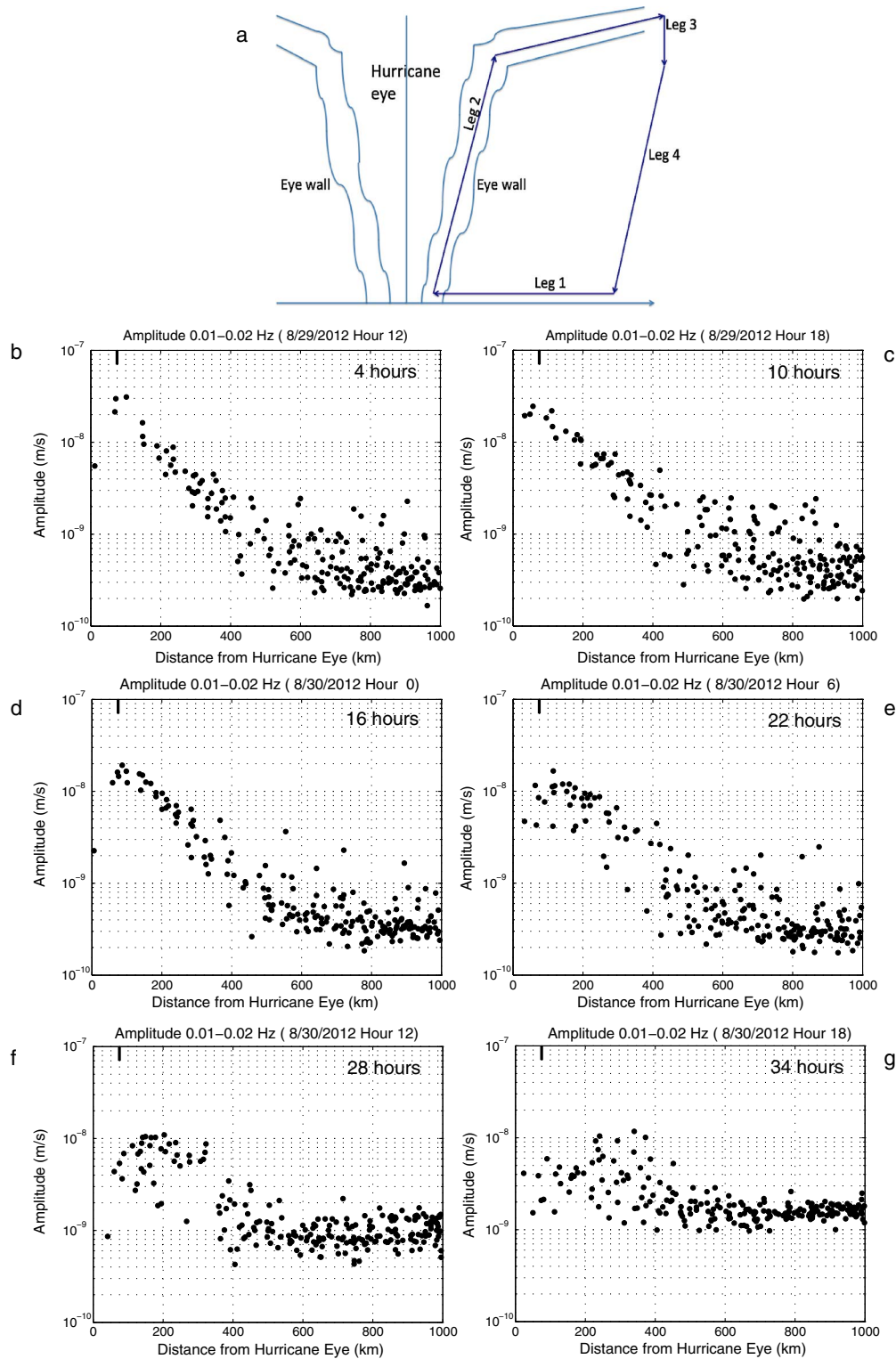


Figure 3. (a) The Carnot-cycle-like airflow for a mature hurricane and (b–g) the seismic amplitude–distance (semilog) plots from the center of Hurricane Isaac after the landfall. The hours indicate the time after the second landfall. Figure 3a shows that there is inflow of air along Leg 1 just above the surface that turns upward at the eyewall and then circulates back through the top of the troposphere. At about the time of landfall (Figure 3b, 4 h later), there is a sharp peak at a distance of 75 km from the center. A short line is given at top at the distance of 75 km. The amplitude peak stays at a similar distance in Figure 3c (10 h later) but may have moved slightly outward in Figure 3d (16 h later). The width of the peak became wider, and the peak values decreased. At later times in Figures 3e (22 h), 3f (28 h), and 3g (34 h), the peak moved away from the center, and the sharpness of the peak disappeared. Higher noise level in Figures 3f and 3g for distances beyond 600 km is due to *M*6.8 earthquake in northern Atlantic but does not affect our analysis.

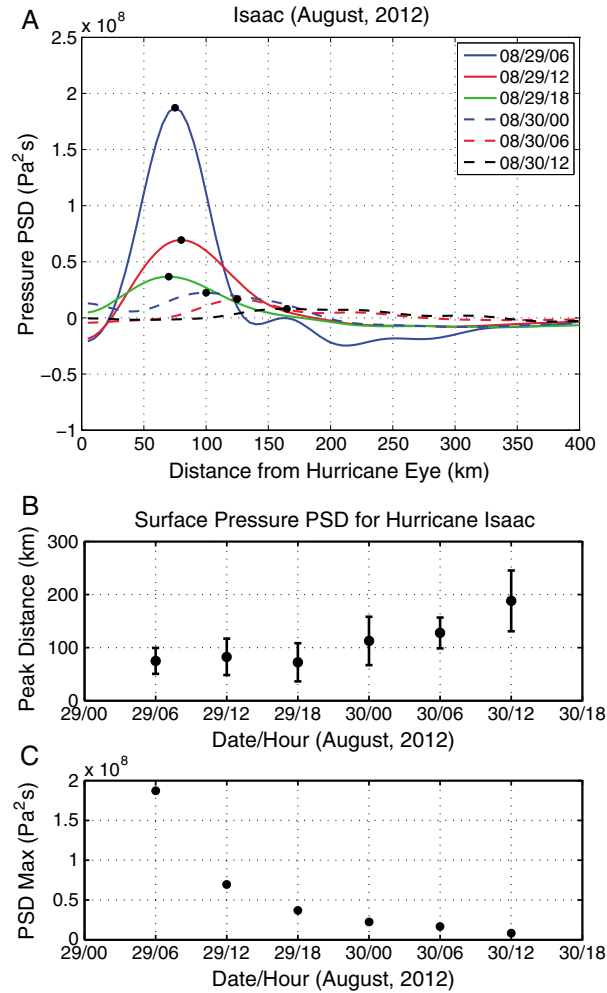


Figure 4. Six pressure PSD solutions and their characteristics. (a) Same six solutions as in Figure 4. The peak of each curve is denoted by a solid circle. The peak basically stayed at similar distances in the first three curves (75, 80, and 70 km; see Table 1), but later, it moved outward from the center. (b) The peak distance from the center and its width (1 sigma; Table 1) are shown. (c) Pressure PSD peak values decreased quickly from the beginning. Pressure PSD became 1/5 after 10 h, or pressure was more than halved after 10 h.

kernel that we can compute for an Earth model. The variable x_s is the source distance from the center of the hurricane, and we assumed that this source was distributed from 10 to 400 km. The kernel formula was derived by using the normal mode theory [Dahlen and Tromp, 1998] and has the form

$$K(x, x_s, \omega) = \frac{\lambda_s^2}{4\pi} R \sin \theta_s \sum_l \sum_{l'} (l' + 1/2)(l'' + 1/2) U_l^2 U_{l'}^2 \gamma_l \gamma_{l'} \int P_{l'}(\cos \Delta') P_{l'}(\cos \Delta') d\phi_s \quad (2)$$

where a continuous, circular source is assumed at distance (radius) x_s (after integration with respect to azimuth ϕ_s). We solved for $S_p(x_s, \omega)$ for the range of $10 \leq x_s \leq 400$ km using the standard preliminary reference Earth model [Dziewonski and Anderson, 1981]. In equation (2), λ_s is the correlation length among surface pressure which we put at 1 km [Herron et al., 1969; McDonald et al., 1971], $\theta_s = x_s/R$ is the angular distance from the hurricane center to a source location (R is the Earth's radius), l' and l'' are the angular degrees of modes, and U_l and $U_{l'}$ are the surface values of vertical eigenfunctions of fundamental modes (we dropped higher modes in the computation as the source is at the surface),

$$\gamma_l = \frac{(\omega_l/2Q_l - i\omega)}{\{(\omega_l/2Q_l - i\omega)^2 + \omega_l^2\}}$$

where Q_l is the attenuation parameter and Δ' is the angular distance between the observation point x and the source x_s . This quantity varies as we perform the integration with respect to ϕ_s .

Table 1. The Information on Isaac in the Left Six Columns is From Berg [2013]^a

Month	Day	Hour	Latitude (North)	Longitude (West)	Central Pressure (hPa)	Max PSD (Pa ² s)	Peak Radius (km)	1 Sigma Range (km)
8	29	06:00	29.1	90.0	966	1.873e8	75.	50.5–99.5
8	29	12:00	29.4	90.5	968	6.937e7	80.	48.2–117.0
8	29	18:00	29.7	90.8	973	3.677e7	70.	36.4–108.4
8	30	00:00	30.1	91.1	977	2.240e7	100.	67.1–158.0
8	30	06:00	30.8	91.5	982	1.669e7	125.	98.5–156.6
8	30	12:00	31.3	91.9	987	0.813e7	165.	130.8–245.3

^aThe maximum PSD (maximum pressure PSD), peak radius, and 1 sigma range are from our seismic data inversion. One sigma range is simply the range where the amplitudes become $1/\sqrt{e}$ of the peak value rather than by formal statistical estimate.

One important caveat is that the above formula shows that only the product of correlation length and the pressure PSD can be constrained by the data. We assume that the correlation length is 1 km, but this value may be different near the center of a hurricane. A different correlation length directly changes pressure estimates. The interpretation of results should be only on the relative changes of pressure and not on the absolute values.

Starting at 6:00 UTC on 29 August, six solutions at every 6 h were obtained. Six solutions for pressure PSD are shown in Figure 4a (top). The maximum values for each solution are indicated by the small solid circles. The first solution shows the peak at the radius of 75 km. Note that cylindrical symmetry for the pressure PSD was assumed for these solutions. Two solutions in the next 12 h show that the cylindrical peaks stayed at about the same radius (80 km and 70 km to be precise). On the other hand, the maximum pressure PSD decreased about fivefold over this 12 h period (Table 1). This means that the surface pressure was slightly more than halved during this period ($1/\sqrt{5}$). We infer that the sharp peak in surface pressure solutions are related to the processes in the eyewall, especially the intensity of ascending flow in it. Nearly stable distances of the pressure peak in Figures 4a–4c imply that the basic structure of the airflow remained for about half a day but with considerable weakening of pressures during this period.

In the next three solutions (Figure 4a) at the 16th, 22nd, and 28th hour after the landfall, the pressure peak moved outward from the hurricane center with further decrease of pressure values. The peaks were found at 100 km, 125 km, and 165 km, and the symmetry about the maximum was lost. There are some indications in the solutions that multiple peaks started to emerge.

While the same features are in Figure 4a, the locations of the maximum values are summarized in Figure 4b, and the decreasing amplitudes of pressure PSD with time are shown in Figure 4c. In the figures in the supporting information, same characteristics of these solutions are displayed from a different perspective (Figure S1 in the supporting information), and the goodness of fit to data can also be examined (Figure S2 in the supporting information).

5. Interpretations and Discussion

From these surface-pressure solutions, we make the following inferences about the behaviors of Hurricane Isaac. At the time of the landfall, the eyewall existed at a distance of about 75 km from the hurricane center. The eyewall remained at this distance from the moving center of the hurricane for approximately 10 h after the landfall; thus, the same air circulation pattern persisted during this period. However, the strength of flow started to decrease right after the landfall. In the following 24 h, the eyewall diffused further and moved outward from the center of the hurricane to a distance of about 200–300 km. At the end of this period (34 h after the landfall), the raw seismic data do not show any systematic, eyewall-like signature. The eyewall must have collapsed completely by the 34th hour. Therefore, the lifetime of the air circulation, that is characteristic for a mature hurricane, was about 1.5 days for Hurricane Isaac.

In this paper, we ignored the effects of horizontal forcing in the formulation for seismic wave excitation by a hurricane. Since the upwelling flow in the eyewall is spatially focused and strong for a mature hurricane, we believe that our assumption of excitation by surface-pressure changes captures the first-order effects, while a hurricane is strong. But it is also true that horizontal shear forcing should make some contributions to seismic signals by a strong, large-scale vortex flow like a hurricane. Its assessment, however, is beyond the scope of this letter and left for a future study.

Acknowledgments

We thank Walter Zuern and an anonymous reviewer for their constructive comments. The first author also thanks a visiting fellowship at the Center for Advanced Study at Ludwig Maximilians University of Munich when this study was concluded. All data were obtained from the data center at IRIS (Incorporated Research Institutions for Seismology). We appreciate accessibility of these data and their efficient service by IRIS.

The Editor thanks Paul Davis and Walter Zuern for their assistance in evaluating this paper.

References

- Berg, R. (2013), Tropical Cyclone Report: Hurricane Isaac (AL092012) 21 August – 1 September 2013, NOAA/National Weather Service, Miami, Fla.
- Bromirski, P. (2001), Vibrations from the "Perfect Storm", *Geochem. Geophys. Geosyst.*, *2*(7), 1030, doi:10.1029/2000GC000119.
- Dahlen, A. F., and J. Tromp (1998), *Theoretical Global Seismology*, Princeton Univ. Press, Princeton, N. J.
- Dziewonski, A. M., and D. L. Anderson (1981), Preliminary reference Earth model, *Phys. Earth Planet. Inter.*, *25*, 297–356.
- Emanuel, K. A. (1986), An air-sea interaction theory for tropical cyclones. Part I: Steady state maintenance, *J. Atmos. Sci.*, *43*, 585–604.
- Emanuel, K. A. (1991), The theory of hurricanes, *Annu. Rev. Fluid Mech.*, *23*, 179–196.
- Emanuel, K. A. (1997), Some aspects of hurricane inner-core dynamics and energetics, *J. Atmos. Sci.*, *54*, 1014–1026.
- Fukao, Y., K. Nishida, N. Suda, K. Nawa, and N. Kobayashi (2002), A theory of the Earth's background free oscillations, *J. Geophys. Res.*, *107*(B9), 2206, doi:10.1029/2001JB000153.
- Hasselmann, K. A. (1963), A statistical analysis of the generation of microseisms, *Rev. Geophys.*, *1*, 177–209, doi:10.1029/RG001i002p00177.
- Herron, T. J., I. Tolstoy, and D. W. Kraft (1969), Atmospheric pressure background fluctuations in the mesoscale range, *J. Geophys. Res.*, *74*, 1321–1329, doi:10.1029/JB074i006p01321.
- Jorgensen, D. P. (1984), Mesoscale and convective-scale characteristics of mature hurricanes. Part I: General observations by research aircraft, *J. Atmos. Sci.*, *41*, 1268–1285.
- Jorgensen, D. P., E. Zipser, and M. A. LeMone (1985), Vertical motions in intense hurricanes, *J. Atmos. Sci.*, *42*, 839–956.
- Longuet-Higgins, M. S. (1950), A theory of the origin of microseisms, *Philos. Trans. R. Soc. London, Ser. A*, *243*, 1–35.
- McDonald, J. A., E. J. Douze, and E. Herrin (1971), The structure of atmospheric turbulence and its application to the design of pipe arrays, *Geophys. J. R. Astron. Soc.*, *26*, 99–106.
- Tanimoto, T. (2005), The oceanic excitation hypothesis for the continuous oscillations of the Earth, *Geophys. J. Int.*, *160*, 276–288.